Molecular dynamics of natural rubber as revealed by dielectric spectroscopy: The role of natural cross–linking

Javier Carretero–González,[ae] Tiberio A. Ezquerra,*[b] Sureerut Amnuaypornsri,[c] Shigeyuki Toki,[d] Raquel Verdejo,[a] Alejandro Sanz,[b] Jitladda Sakdapipanich,[c] Benjamin S. Hsiao[d] and Miguel A. López–Manchado[a]

Received 15th February 2010, Accepted 14th April 2010
DOI: 10.1039/c003087b

In order to understand the molecular dynamics of natural rubber, the dielectric relaxation behavior of its different components were investigated. These components included: (1) the linear polyisoprene fraction, obtained after deproteinization and transesterification of natural rubber (TE–DPNR), (2) the gel (GEL) fraction, corresponding to pure natural chain–end cross–linked natural rubber, (3) deproteinized natural rubber (DPNR), in which the protein cross–links at the ω–end have been removed, and (4) natural rubber (CNR) purified (through centrifugation) but still containing proteins, phospholipids and the sol phases. The dielectric relaxation behaviour of natural rubber revealed a segmental mode (SM) which is not affected by natural chain-end cross-linking (so-called naturally occurring network) and a normal mode (NM) which depends on a naturally occurring network. The dynamics of the NM, which is associated to chain mobility, seems to be strongly affected by natural chain-end cross-linking. We propose a model based on a hybrid star polymer in which the low mobility core (phospholipids) controls the mobility of the polyisoprene arms.

A. Introduction

Natural Rubber (NR) is a complex biomaterial mainly composed of a linear chain formed by two *trans*-1,4 isoprene units and between 10^3 and $3\bullet10^3$ *cis*-1,4 isoprene units.[1–3] The linear isoprene chain is terminated in one end, the so called α–terminal, by a mono- or di-phosphate group, linked with phospholipids.[1–3] The other end, referred to as the ω–terminal, has been postulated to be a modified dimethylallyl unit linked with a functional group, which can be associated with proteins to form cross–links through intermolecular hydrogen bonding. Additionally, NR contains significant amounts of proteins and lipids as a result of the biosynthesis mechanism of rubber formation.[1] The presence of proteins and phospholipids in NR induces a multi-scaled microstructure characterized by natural cross–linking among the terminal groups of linear polyisoprene chains. Proteins are responsible for the cross–linking of ω–terminals by means of hydrogen bonding, while interactions among phospholipids provide cross–linking of α–terminals. This type of microstructure forms the gel phase of natural rubber, schematized in Fig. 1, which coexists with the sol phase mainly compose by uncross–linked material.[1–6]

Natural impurities can connect the linear polyisoprene segments in NR through functional terminals and generate the following different chain formations like those indicated in Fig. 1: A) extension of a linear chain, B) branching of three chains, C) star formation of multi chains. The combination of all of them can form a network. In addition, phospholipid natural impurities can also generate micelles and proteins can generate aggregates (see Fig. 1). Different chain connections lead to formations of branch, star and network structures, which are termed the "naturally occurring network".[6] This unique micro-structure endows NR mechanical properties not achievable by its synthetic analogues, making NR one of the most fascinating and important industrial natural polymers among engineering plastics. Although the real cross-linking structure and role of proteins are not fully understood, it was suggested that the cross–linking of NR formed by proteins can be eliminated by deproteinization and that formed by phospholipids can be eliminated by transesterification. The combination of both chemical processes leads to obtain linear NR. The effect of proteins and

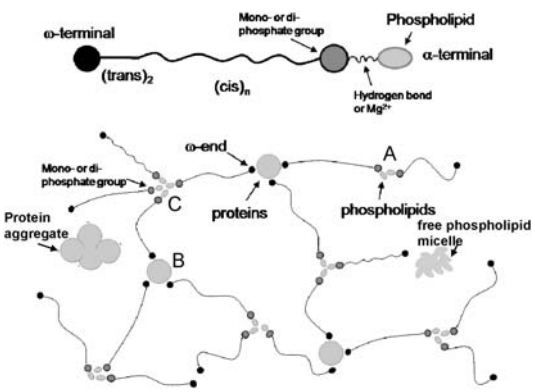

Fig. 1 Proposed structure of natural rubber (NR) occurring network.[1–6]

[a]*Instituto de Ciencia y Tecnología de Polímeros, CSIC, Juan de la Cierva 3, 28006, Madrid, Spain*
[b]*Instituto de Estructura de la Materia, CSIC, Serrano 119, 28006 Madrid, Spain*
[c]*Department of Chemistry and Center of Excellence for Innovation in Chemistry, Mahidol University, Bangkok, 10400, Thailand*
[d]*Department of Chemistry, Stony Brook University, Stony Brook, New York, 11794-3400*
[e]*The Alan G. MacDiarmid Nanotech Institute, University of Texas at Dallas, Richardson, TX, 75083, USA*

phospholipids on strain induced crystallization and the correlation with the tensile strength of NR have been extensively studied by X-ray diffraction and microscopic methods.[6,7] However, to our knowledge, there is a lack of systematic investigation on how the natural impurities, which control the microstructure of NR, affect the molecular dynamics of rubber chains. Most of the studies dealing with the dynamics of polyisoprene (PI) have been accomplished in synthetic samples and only a few in natural rubber.[8–11] The dielectric behavior of *cis*–polyisoprene is characterized by a strong relaxation, related to segmental motions, which appears at temperatures above the glass transition (T_g). Additionally, due to its chemical structure, *cis*-PI is a type A polymer (see scheme in Fig. 2) with a electrical dipole component parallel to the chain backbone.[12] Therefore, there is a slower dynamics, referred to as the normal mode (NM), that is related to the end-to-end relaxation of dipole moment of the *cis*–PI chain.[13–16] Consequently, the normal mode is related to the chain dynamics and is strongly dependent on the molecular weight.

In this work, we use broadband dielectric spectroscopy to study the segmental and chain dynamics of NR with different levels of cross–linking, induced by the selective elimination of proteins and phospholipids aiming to characterize dynamically the influence of natural cross–linking agents. We have investigated NR with different microstructures including: (a) centrifuged natural rubber (CNR) in which free non-rubber components are eliminated by centrifugation, (b) the non soluble phase in toluene (GEL), (c) deproteinized natural rubber (DPNR) in which free proteins are removed and (d) transesterified and deproteinized natural rubber (TE-DPNR) which is composed of linear polyisoprene chains. The main aim of the study is to identify the segmental and chain relaxation mechanisms which are influenced by the natural cross-linking.

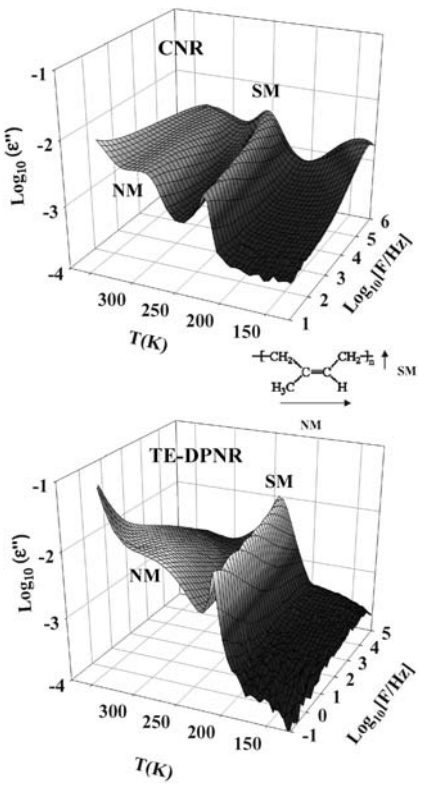

Fig. 2 3D plot of the frequency and temperature dependence of the dielectric loss, ε'', for CNR (top) and TE–DPNR (bottom) samples.

B. Experimental

B.1. Sample preparation

Natural rubber (NR) latex used in this study was obtained from regularly tapped Hevea tree of RRIM 600 clone, provided by the Thai Rubber Latex Co., Thailand. A systematic procedure to separate the different natural rubber components was accomplished according to the following steps:

1. Raw natural rubber latex was centrifuged at a speed of 13,000 rpm for 30 min in order to remove sludge and water soluble impurities, such as amino acids, sugars and metal ions. The cream fraction was collected and dried in an oven at 323 K. This material is referred to as centrifuged natural rubber (CNR).

2. CNR was subsequently dissolved in toluene solution at a concentration of 1 wt%. This solution was kept in the dark without stirring for a week. Then, the gel fraction (GEL) was separated from the sol fraction by centrifugation at a speed of 10,000 rpm for 30 min. The gel fraction was collected and dried in a vacuum oven at 313 K. The lighter part is the sol fraction, about 80%, which is composed of toluene soluble rubber and soluble natural impurities. The gel fraction contains insoluble rubber and insoluble natural impurities.

3. Deproteinized NR (DPNR) was prepared by incubation of NR latex (30% weight/volume (w/v) dry rubber content) with 0.04% w/v proteolytic enzyme (KAO KP-3939) and 1% w/v Triton® X–100 for 12 h at 310 K followed by centrifugation at 13,000 rpm for 30 min. The cream fraction was re-dispersed with 0.5% w/v Triton® X-100 to make 30% w/v dry rubber content and re–centrifuged at 13,000 rpm for 30 min. This process eliminates the protein content.[1]

4. Finally, transesterified and deproteinized NR (TE–DPNR) was prepared by the reaction of DPNR with freshly prepared sodium methoxide in toluene solution at room temperature for 3 h, followed by precipitation using an excess amount of methanol. This process eliminates the phospholipid content.[1]

The molecular weight of the rubber samples was determined by size exclusion chromatography (JASCO-Borwin) using two columns in line, packed with crosslinked polystyrene gel having the exclusion limits of $2\bullet10^7$ and $4\bullet10^5$ g mol^{-1}. The rubber solution was prepared by dissolving rubber into tetrahydrofurane (THF) (LabScan, HPLC grade) at the concentration of 0.05% (w/v) and filtered through a Millipore prefilter and 0.45 μm membrane filter (Alltech). THF was used as eluent with a flow rate of 0.5 ml min^{-1} at 308 ± 0.01 K, monitoring with refractive index as a detector. Commercially available *cis*–1,4 polyisoprene (Polymer Standard Service GmbH, Germany) was

Table 1 Insoluble fraction in THF and molecular weight of NR samples

Samples	Insoluble fraction in THF (%w/w)	M_w (× 10^6)	M_n (× 10^5)	M_w/M_n
CNR	30.7	1.87	2.87	6.53
DPNR	4.4	2.16	3.29	6.56
TE–DPNR	~0	1.46	2.84	5.13

used as standard sample of the molecular weight. Data of the molecular weight of the different samples is included in Table 1.

B.2. Dielectric spectroscopy and data analysis

Dielectric loss measurements (ε'', where $\varepsilon'' = \mathrm{Im}\,(\varepsilon^*)$ with ε^* being the complex dielectric permittivity) were performed over a broad frequency range (10^{-1} Hz < F (Hz) < 10^7 Hz) in a temperature range of 123 K < T < 373 K using a BDS–40 NOVOCONTROL system with an integrated dielectric interface ALPHA and a QUATRO temperature controller. The temperature in these experiments was controlled by a nitrogen jet, thus having a temperature error of ±0.1 K during every single sweep in frequency. Samples for dielectric measurements were dissolved in a toluene solution at a concentration of 4% w/w. The solution was cast using a dropper on a golden disc (3 cm in diameter, by NOVOCONTROL), which was used as the lower electrode. The electrode was rotated and inclined manually in order to cover homogeneously the electrode surface. Subsequently, the samples over the electrode were dried at 313 K in vacuum. A smaller golden electrode of 2 cm (NOVOCONTROL) was placed on top of the sample. Due to the viscous nature of the samples, the thickness could no be accurately defined over the whole temperature range covered by the measurements. For this reason discussion of the dielectric data was based on the maxima of the relaxation curves rather than on the dielectric strength values. The observed normal and segmental relaxations were analyzed using procedures described elsewhere,[15,17] which involve the use of the phenomenological Havriliak-Negami (HN) equation containing a conductivity term. Since $\varepsilon'(\omega)$ and $\varepsilon''(\omega)$ are related to each other *via* the Kramers–Kronig relation,[17] the functional form of the HN description was used to evaluate $\varepsilon''(\omega)$ values over the entire relaxation range. The experimental data have been described by the empirical equation of HN:

$$\varepsilon'' = \mathrm{Im}\left[\varepsilon^*\right] = \mathrm{Im}\left[\varepsilon_\infty + \sum_{x=I,II} \Delta\varepsilon_x \left[1 + (i\omega\tau_x)^{b_x}\right]^{-c_x}\right] + \left(\frac{\sigma_{dc}}{\varepsilon_{VAC}\omega}\right)^s \quad \text{(eq.1)}$$

where I and II indicate the segmental and normal mode relaxations, $\omega = 2\pi F$, $\Delta\varepsilon_x$ is the dielectric strength, τ_x is the central relaxation time of the relaxation time distribution function, and b and c (0 < b, c < 1) are the shape parameters which describe the symmetric and asymmetric broadening of the relaxation time distribution function, respectively. Here, σ_{dc} is related to the direct current electrical conductivity, ε_{VAC} is the vacuum dielectric constant, and s depends on the nature of the conduction mechanism. The relaxation time corresponding to the maximum in ε'' can be estimated by:[17,18]

$$\tau_{max} = \tau_{HN}\left[\sin\left(\frac{b\pi}{2+2c}\right)\right]^{-\frac{1}{b}}\left[\sin\left(\frac{bc\pi}{2+2c}\right)\right]^{\frac{1}{b}} \quad \text{(eq.2)}$$

C. Results

C.1. Dielectric relaxation behaviour

While CNR can be considered to be a purified natural rubber cross-linked at the chain ends by natural agents (see Fig. 1),

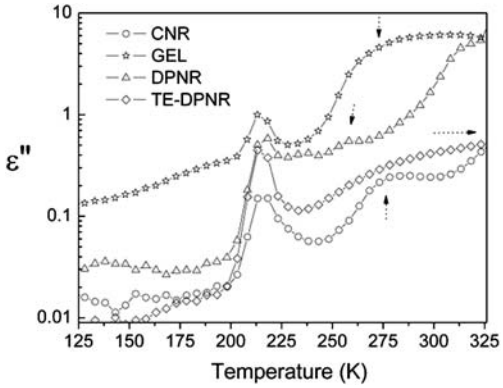

Fig. 3 Temperature dependence of the dielectric loss, ε'', at 7 Hz for: (o) (CNR), (☆) (GEL), (△) Deproteinized natural rubber (DPNR) and (◇) (TE–DPNR). The arrows are an indication of the location of the NM process.

TE–DPNR corresponds to the non cross–linked linear natural polyisoprene. Fig. 2 shows the temperature and frequency dependence of the dielectric loss ε'' for CNR and for TE–DPNR. As expected, the measurements exhibit a low–temperature process just above the glass transition temperature ($T_g \sim 213$ K), which can be assigned to the segmental–mode process (SM). Similarly as for synthetic polyisoprene, it originates from local motions of the perpendicular dipole moment.[15] A broader relaxation is detectable at higher temperatures in both samples which, again similarly to the synthetic polyisoprene case, can be assigned to the normal–mode process (NM). The NM process, detectable because of the dipole component parallel to the backbone, corresponds to motions of the entire chain.[8,9,15] This general relaxation behavior is qualitatively similar for all the samples investigated. For the sake of comparison, Fig. 3 illustrates the dependence of ε'' at 7 Hz as a function of temperature. In this Figure, the segmental–mode appears as a relatively sharp maximum, while the normal–mode appears as a broader one at higher temperatures. It is evident that the position of the maximum in ε'' SM does not vary from sample to sample. On the contrary, the NM exhibits significant variation with different sample treatment. According to these data, the NM for

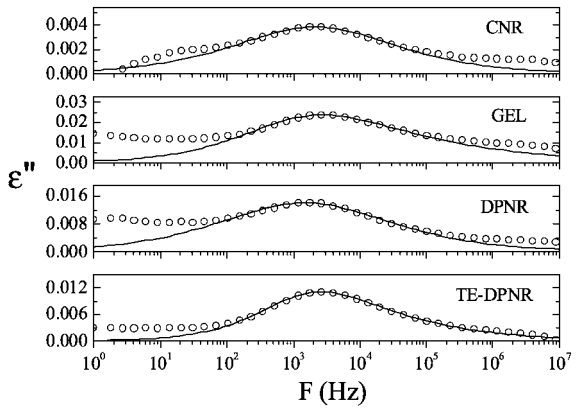

Fig. 4 Dielectric loss, ε'', for CNR, GEL, DPNR and TE–DPNR samples as a function of frequency, F (Hz), at 223 K for the segmental mode (SM). The continuous lines represent best fit to the eqn (1).

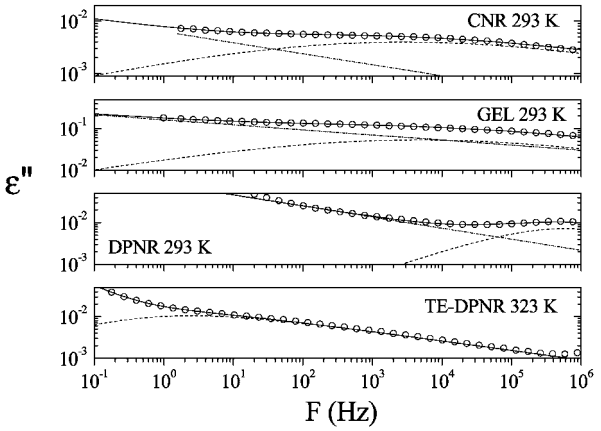

Fig. 5 Dielectric loss, ε″, for CNR, GEL, DPNR and TE–DPNR samples as a function of frequency, F (Hz), at selected temperatures where the NM is well resolved. The continuous lines represent best fit to eqn (1).

TE–DPNR seems to be slower than that of CNR. The NM for the DPNR sample is not well resolved in the isochronal plot, shown in Fig. 3, therefore isothermal representations are necessary. Fig. 4 and 5 illustrate selected isothermal plots of ε″ as a function of frequency corresponding to the SM (Fig. 4) and NM (Fig. 5) for the different samples. As far as the SM is concerned, the data in Fig. 4 clearly show that the maximum in ε″ is not significantly affected by the sample treatment. Fig. 5 shows isothermal plots in the temperature region where the NM appears for the different samples. Contrary to what was observed for the SM, a significant variation with sample treatment is seen for the NM. The results of Fig. 5 clearly show that the NM of the GEL sample becomes slightly faster than that of CNR. Moreover, the NM for the DPNR is even faster than that of the GEL sample. On the contrary, the NM of the TE–DPNR sample is the slowest one of all the investigated samples.

C.2. Relaxation times for segmental and normal modes

It was possible to analyze the two relaxation processes individually for all the samples. For this purpose, the loss curves were resolved into two contributions from normal and segmental modes, respectively. Since the dielectric curves are in general broad and asymmetric, the HN function (eqn (1)) was used to fit the data.[15,17,19] The continuous lines of Fig. 4 show that the HN function gives a reasonable description of the experimental data for the segmental mode. In these cases, only one relaxation term was considered to contribute to eqn (1). The corresponding fitting parameters are collected in Table 2.

Table 2 Parameters of the HN equation for the Segmental mode (SM)

Sample	T/K	b	c	τ_{HN}/s
CNR	223	0.50	1	$7.5\ 10^{-4}$
GEL	223	0.58	0.51	0.0017
DPNR	223	0.46	0.98	0.0011
TE–DPNR	223	0.55	0.7	0.0013

Table 3 Parameters of the HN Equation for the Normal mode (NM)

Sample	T/K	b	c	τ_{HN}/s
CNR	293	0.26	0.8	0.00126
GEL	293	0.26	1	3.3×10^{-4}
DPNR	293	0.56	1	2.5×10^{-6}
TE–DPNR	323	0.5	0. 46	0.28

The analysis of the NM data is more complex because of the segmental mode contribution at high frequencies and of the conductivity term that affects the low frequency tail of the relaxation curves. For this reason, eqn (1) was used for two relaxations, one for SM and other for NM, all having an additional conductivity term to fit the data in the temperature range where the NM is analyzed. The SM mode relaxation at high temperatures can be simulated by extrapolation of the HN parameters fitted at lower temperatures.[20,21] The continuous lines of Fig. 5 show the fit of the HN function to the experimental data indicating the contribution of the different terms of eqn (1). The corresponding shape parameters are collected in Table 3.

The fitting procedure was performed in the whole temperature range for all the samples. By this procedure, the temperature dependence of the relaxation time associated to the maximum in ε″ can be calculated according to eqn (2). Fig. 6 shows the average relaxation time (eqn (2)) as a function of reciprocal temperature for both SM and NM processes and for all the investigated samples. In all cases, the temperature dependence of the relaxation time departures from the simple Arrhenius behavior exhibiting a curvature at high temperatures. This characteristic temperature dependence, which generally characterizes both segmental and normal modes,[8,9,15] can be described by means of the Vogel–Fulcher–Tammann (VFT) equation:

$$\tau_{max} = \tau_0 \exp[A/(T - T_0)] \qquad \text{(eq. 3)}$$

where τ_0, T_0 and A are constants with $T_0 < T_g$. As far as the segmental mode is concerned, the parameter A can be redefined as $A = D \bullet T_0$, where D is referred to as the fragility strength

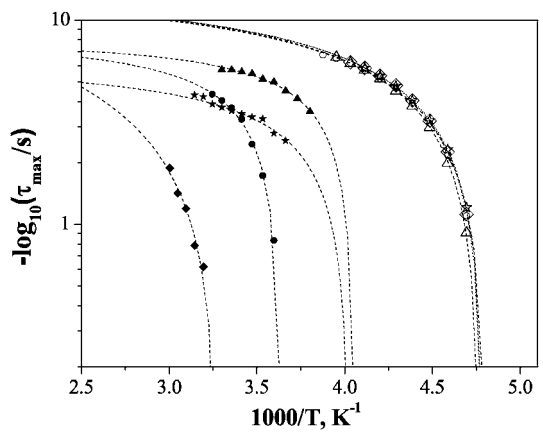

Fig. 6 Activation plot for the segmental (hollow symbols) and the normal (solid symbols) modes for: (○, ●) CNR, (★, ☆) GEL, (△, ▲) DPNR and (◇, ◆) TE–DPNR samples. The dotted lines represent the fits of eqn (3).

Table 4 VFT parameters for the segmental and normal mode processes

	segmental mode		normal mode	
Sample	D	T_0/K	A/K	T_0/K
CNR	4.52	157.3	218.4	247.7
GEL	4.17	160.6	191.9	216.5
DPNR	4.22	161.1	161.1	226.3
TE–DPNR	4.27	161.0	2609.3	119.1

parameter that can be related to the characteristics of segmental motions above the glass transition temperature.[22] The dashed lines in Fig. 6 indicate the fittings of the VFT equation to the experimental data. The fitting parameters are reported in Table 4.

D. Discussion

The results presented until now seem to indicate that dielectric spectroscopy is a useful technique to deal with the molecular dynamics of natural rubber specimens with different structural hierarchy. The starting step for the discussion will be to consider the chosen polymer system is a cross–linked polymer network, where cross–links affect essentially the motions of chain ends. While the deproteinization treatment tends to eliminate the cross–linking in the ω–terminal chain ends, the transesterification process tends to eliminate cross–links in the α–terminal ones. Consequently, the combination of deproteinization and transesterification treatments render to natural linear polyisoprene.[1–3] Analogously to synthetic polyisoprene,[8,9,15] the general relaxation behaviour of the different rubber samples exhibit two processes (Fig. 2).

D.1. Segmental mode of natural rubber

Starting from lower temperatures, the segmental mode (SM) appears above the glass transition temperature and can be attributed to segmental motions of polymer chains.[8,9,15] For synthetic polyisoprene, the SM does not depend on the molecular weight.[15] In our case, according to the relaxation time date shown in Fig. 6, the SM does not depend on the treatment given to samples. Dielectric experiments performed in polymer networks have shown that the α–relaxation, attributed to the segmental mode, depends on network density and shifts toward higher temperatures as the cross–link density increases.[23,24] However, the nature of the cross–linking in natural rubber is very peculiar as it concerns exclusively the chain ends (Fig. 1). Therefore, in this case, modification of the cross–linking of natural rubber by the different treatments does not significantly affect segmental motions since the molecular weight among cross–links is very high, of the order of 10^6 g mol^{-1}. The value of the fragility strength parameter, D, does not vary with sample treatment. The D value around 4 indicates that natural rubber is a dynamically fragile system as corresponds in general to polymer materials.[25]

D.2. Normal mode of natural rubber

Besides the segmental mode, all the investigated samples exhibit at higher temperatures a broad process (Fig. 2 and 3) which, in analogy to what it has been reported for synthetic polyisoprene, can be attributed to a normal mode.[8,9,15] The normal mode (NM) appears as a consequence of the chemical structure of the *cis*–polyisoprene chain that has components of the dipole moment parallel to the chain contour.[15] Therefore, *cis*–polyisoprene can exhibit a dielectric NM process caused by the parallel dipole moment in addition to the common SM process mainly originated by molecular motions affecting the perpendicular dipole moment. The main effect observed in the dynamics of the NM for the different samples is the dependence of chain mobility with the chain-end cross-linking (Fig. 6). Basically, TE-DPNR with no chain-end cross–linking exhibits slower chain dynamics than the GEL, with cross–linking in the α– and ω–chain ends while DPNR exhibits the faster dynamics.

The slower NM exhibited by the TE-DPNR sample (Fig. 6) can be essentially considered to be analogous to that exhibited by a linear polyisoprene.[1–3] However, the relaxation time of 0.28 s at 323 K for the TE-DPNR sample (Table 3) is about three orders of magnitude faster than the relaxation time predicted for synthetic polyisoprene.[15] Somehow this is expected since the reported results for synthetic polyisoprene refer to samples with very narrow polydispersity[15] ($M_w/M_n \approx 1$). In this study, natural rubber samples exhibits much broader polydispersities close to 6 (Table 1). Therefore, the presence of low molecular components may affect significantly the average relaxation time.

The deproteinized natural rubber (DPNR) sample is mainly cross-linked by phospholipids at α–terminal chain ends. Therefore, in this study we can consider DPNR as a star polymer,[26] in which the centre of the star has a different nature as that of the star arms. The dynamics of star polymers in general and of polyisoprene stars in particular have been investigated by dielectric spectroscopy.[26,27] It has been proposed that the motion of star polymers should be around four times slower than that of free linear chains of similar length as those in the star arms.[28] This hypothesis was corroborated by dielectric relaxation measurements for synthetic *cis*–polyisoprene stars.[26] In these studies, the NM of the polymer stars is shown to be significantly slower than that of the corresponding arms.[26] This effect seems, at first glance, to contradict the observation in this study, since the NM of DPNR is much faster than that of TE-DPNR (Fig. 6).

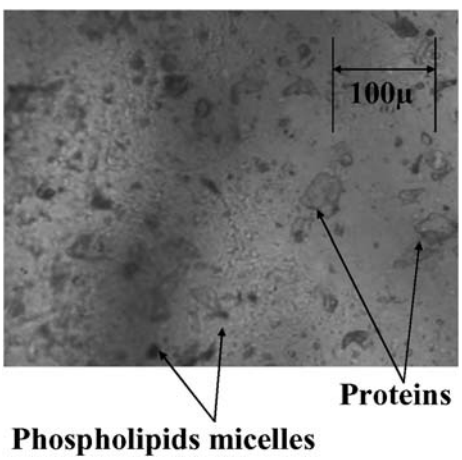

Fig. 7 Optical micrograph of natural rubber indicating the presence of proteins aggregates and phospholipids micelles.

Faster NM processes in *cis*–polyisoprene stars than those of the linear arms have been observed under confinement.[29] Dielectric spectroscopy was used to study the NM of polyisoprene in microphase separated star diblock copolymers where polyisoprene forms a core and polystyrene forms a corona.[29] According to Floudas *et al.*,[29] the NM process is strongly influenced by the spatial confinement induced by the polystyrene phase. This phase confines the polyisoprene star centre within an effective radius R such that $<(\triangle R)^2>^{1/2} \approx b(M_e)^{1/2}$, where b is the statistical segment length ($\approx$ 0.68 nm for PI) and M_e is the molecular weight among entanglements. The main effect is the enhancement of polyisoprene chain mobility. This has been explained considering that the dielectric NM is mainly determined by the motion of the central part of the star.[29] Calculations based on the Rouse model[29] indicated that the NM process in the star can become faster than that of the arm if $M > 1.5\ M_e$ where M is the arm molecular weight. Inspired by these ideas, we have attempted to explain the enhanced NM dynamics of DPNR as compared to that of TE-DPNR. In the chosen system, DPNR can be considered as a hybrid star polymer because the core of the star, formed by a phospholipid aggregate, is chemically different from the arms. This chemical heterogeneity is expected to make the molecular mobility of the phospholipid core to be very different from that of the polyisoprene arms. The optical micrography of natural rubber samples shown in Fig. 7 indicates the presence of phospholipids micelles with sizes as large as $\approx$ 10 μm. This suggests that the phospholipids core should be very effective in fixating the α-terminal chain ends. We propose that the phospholipid core has, at least due to its size, a restricted mobility as compared with that of the arms. While in the case discussed by Floudas *et al.*, the PS confining phase restricts the mobility of the star centre, in our case it is the chemical heterogeneity of the hybrid star in its core the responsible for the restricted mobility around the arm α-end regions. Additionally, there exists a topological confinement induced by the entanglements.[29] This effect is expected to be very significant considering that the molecular weight of the polyisoprene arms is about three orders of magnitude higher than M_e. Due to entanglement constraints, the star centre would not be free to explore the whole space, since moving through one tube would provoke modification of the tube diameter to accommodate the hybrid core. Due to this restricted situation, the star centre tends to be localized. According to Floudas *et al.*[29] the ratio between the relaxation time of the star polymer, τ_{star}, and that of the arm, τ_{linear}, for a homogeneous, *i.e.* not hybrid, star should follow that:

$$\frac{\tau_{star}}{\tau_{linear}} \alpha \left(\frac{M_e}{M}\right)^3 \qquad \text{(eq. 4)}$$

where M is the molecular weight of the arm and M_e is the molecular weight among entanglements and the proportionality constant is the number of arms. This relation predicts that the chain relaxation mode would become faster when $M > 1.5M_e$. Considering the molecular weight of the linear polyisoprene (TE-DPNR) $\approx 10^6$ and that of M_e for natural polyisoprene[30] $\approx 3\bullet10^3$, a significantly faster dynamics could be expected for DPNR as compared to that of TE-DPNR as experimentally observed.

The Gel component of natural rubber consists essentially of a natural network with cross–links at both chain–ends (Fig. 1). The chain dynamics of the GEL samples is slightly slower than that of DPNR but still significantly faster than that of the TE–DPNR sample. Considering the arguments provided in the previous sections, this effect can be understood because the mobility of polyisoprene arms of the DPNR hybrid star becomes, in the GEL, more restricted due to the additional fixation of their free ω–ends by the protein components (Fig.1). The aggregates of proteins can also be of the order of tens of μm and therefore also very effective in fixating the ω–terminals chain–ends. However, in spite of this, the chain dynamics of the Gel sample remains faster than that of the TE–DPNR linear polyisoprene sample. This indicates that the chain dynamics of the GEL component is dictated by the relaxation at the cores of two different hybrid stars associated to the different chain ends of natural polyisoprene.

The chain dynamics of natural rubber (CNR) presents a NM which is located close to that of the GEL and in between those of TE-DPNR and DPNR (Fig. 6). This can be understood considering the heterogeneous nature of CNR, which consists of a pure network fraction, the GEL component, and a Sol fraction composed of branched polymer and linear chain. Accordingly, it is expected that chain dynamics reflects features of both components. At high temperatures, the NM relaxation times practically overlap those of the GEL component indicating the fast dynamics of both cores of the hybrid stars, α–ends and ω–ends, which control the overall chain relaxation behavior. At lower temperatures, the NM of CNR tends to become slower than that of the GEL component probably due to the contribution of the linear polyisoprene sol component, which seems to dominate at low temperatures the overall CNR chain dynamics with slower modes.

Conclusions

The results presented in this study show that in order to understand the molecular dynamics of natural rubber it is necessary to take into consideration the complexity of this natural material. This can be accomplished by investigating the dielectric relaxation of the different components in natural rubber. In this work, we have investigated by dielectric spectroscopy the relaxation behavior of: (1) the linear polyisoprene component, obtained after deproteinization and transesterification of natural rubber (TE-DPNR), (2) the gel fraction, which correspond to pure natural chain-end cross–linked natural rubber, (3) a deproteinized natural rubber (DPNR) sample, in which the protein cross–links at the ω–end have been removed, and (4) a natural rubber sample (CNR) purified by centrifugation which contains the protein, phospholipids, the gel and the sol phases. The general relaxation behaviour of the different rubber components exhibit two processes: the segmental mode (SM), attributed to the segmental motions of the polymer chains, and a normal mode (NM) associated with the chain dynamics. While the SM does not depend on the treatment of the sample, a significant effect is observed for the NM. The main effect observed in the dynamics of the NM for the different samples is the dependence of the chain mobility with the chain end cross–linking. TE–DPNR, with essentially no chain-end cross–linking, exhibits a slower chain dynamics than that of the GEL, with cross–linking in the α– and ω–chain-ends. DPNR exhibits the fastest dynamics. This

effect has been explained considering DPNR as a hybrid star polymer in which the core and the arms have different chemical nature. The faster chain dynamics of DPNR can be understood as caused by the restricted mobility of the phospholipids core. The chain dynamics of the GEL sample slows down as a consequence of the restricted mobility of polyisoprene arms of the DPNR hybrid star induced by the fixation of their free ends due to the protein component. However, the chain dynamics of the GEL remains significantly faster than that of the TE–DPNR linear polyisoprene sample. Finally chain dynamics of natural rubber (CNR) is located close to that of the GEL and in between those of TE–DPNR and DPNR. This has been explained considering the heterogeneous nature of CNR which consist of a pure network fraction, the GEL component, and a linear polyisoprene fraction, the Sol. At high temperatures the chain relaxation of CNR is caused by the dynamics of both cores of the hybrid stars, α–ends and ω–ends, while at lower temperatures the linear polyisoprene sol component tends to slow down the overall CNR chain dynamics.

Acknowledgements

We thank the financial support from MAT2007-61116 and MAT2009-07789 (MICINN) Spain for generous support of this investigation. J. C. G. acknowledges support from MICINN in the form of a FPI grant. The authors would like to appreciate the support from the Center of Excellence for Innovation in Chemistry (PERCH-CIC), Thailand. The US team thanks the financial support by the National Science Foundation (DMR-0906512). A. S. acknowledges CSIC for a JAE-doc tenure.

References

1 Y. Tanaka, *Rubber Chem. Technol.*, 2001, **74**, 355–375.
2 S. Amnuaypornsri, J. Sakdapipanich, S. Toki, B. S. Hsiao, N. Ichikawa and Y. Tanaka, *Rubber Chem. Technol.*, 2008, **81**, 753–766.
3 S. Amnuaypornsri, J. Sakdapipanich and Y. Tanaka, *J. Appl. Polym. Sci.*, 2009, **111**, 2127–2133.
4 S. Toki, I. Sics, B. S. Hsiao, S. Murakami, M. Tosaka, S. Poompradub, S. Kohjiya and Y. Ikeda, *J. Polym. Sci., Part B: Polym. Phys.*, 2004, **42**, 956–964.
5 J. Rault, J. Marchal, P. Judeinstein and P. A. Albouy, *Macromolecules*, 2006, **39**, 8356–8368.
6 S. Toki, C. Burger, B. S. Hsiao, S. Amnuaypornsri, J. Sakdapipanich and Y. Tanaka, *J. Polym. Sci., Part B: Polym. Phys.*, 2008, **46**, 2456–2464.
7 J. Carretero-Gonzalez, R. Verdejo, S. Toki, B. S. Hsiao, E. P. Giannelis and M. A. Lopez-Manchado, *Macromolecules*, 2008, **41**, 2295–2298.
8 K. Adachi and T. Kotaka, *Macromolecules*, 1984, **17**, 120–122.
9 K. Adachi and T. Kotaka, *Macromolecules*, 1985, **18**, 466–472.
10 S. Cerveny, R. Bergman, G. A. Schwartz and P. Jacobsson, *Macromolecules*, 2002, **35**, 4337–4342.
11 P. Janik, M. Paluch, J. Ziolo, W. Sulkowski and L. Nikiel, *Phys. Rev. E: Stat., Nonlinear, Soft Matter Phys.*, 2001, **64**, 042502.
12 A. Schonhals and R. Stauga, *J. Chem. Phys.*, 1998, **108**, 5130–5136.
13 B. T. Poh, K. Adachi and T. Kotaka, *Macromolecules*, 1987, **20**, 2574–2579.
14 K. Adachi and T. Kotaka, *Prog. Polym. Sci.*, 1993, **18**, 585–622.
15 D. Boese and F. Kremer, *Macromolecules*, 1990, **23**, 829–835.
16 J. Mijovic, H. K. Lee, J. Kenny and J. Mays, *Macromolecules*, 2006, **39**, 2172–2182.
17 K. F. A. Schönhals, *Broad Band Dielectric Spectroscopy*, Springer-Verlag, Berlin, 2002.
18 R. Richert and C. A. Angell, *J. Chem. Phys.*, 1998, **108**, 9016–9026.
19 S. Havriliak and S. Negami, *Polymer*, 1967, **8**, 161.
20 J. C. Coburn and R. H. Boyd, *Macromolecules*, 1986, **19**, 2238–2245.
21 A. Nogales, Z. Denchev, I. Sics and T. A. Ezquerra, *Macromolecules*, 2000, **33**, 9367–9375.
22 C. A. Angell, *Polymer*, 1997, **38**, 6261–6266.
23 K. L. Ngai and C. M. Roland, *Macromolecules*, 1994, **27**, 2454–2459.
24 V. Y. Kramarenko, T. A. Ezquerra, I. Sics, F. J. Balta-Calleja and V. P. Privalko, *J. Chem. Phys.*, 2000, **113**, 447–452.
25 R. Bohmer, K. L. Ngai, C. A. Angell and D. J. Plazek, *J. Chem. Phys.*, 1993, **99**, 4201–4209.
26 D. Boese, F. Kremer and L. J. Fetters, *Macromolecules*, 1990, **23**, 1826–1830.
27 C. M. Roland and C. A. Bero, *Macromolecules*, 1996, **29**, 7521–7526.
28 W. W. Graessley, *Adv. Polym. Sci.*, 1982, **47**, 67–117.
29 G. Floudas, S. Paraskeva, N. Hadjichristidis, G. Fytas, B. Chu and A. N. Semenov, *J. Chem. Phys.*, 1997, **107**, 5502–5509.
30 L. J. Fetters, D. J. Lohse, D. Richter, T. A. Witten and A. Zirkel, *Macromolecules*, 1994, **27**, 4639–4647.

